R.Pöschl, J.Woisetschläger, H.Jericha (1999) *Erosion due to particle impact in supersonic flow*, IMech Conference Transactions, 3rd European Conference on Turbomachinery, Vol.A *Fluid Dynamics and Thermodynamics*, IMechE 1999-1A C557/091/99, pp 405-415

EROSION DUE TO PARTICLE IMPACT IN SUPERSONIC FLOW

R. PÖSCHL, J. WOISETSCHLÄGER, H. JERICHA

Institute for Thermal Turbomachinery an Machine Dynamics
University of Technology, Graz, Austria

1. <u>ABSTRACT</u>

The paper has the intention to clear up the mechanics of erosion at high velocity impact at flat impact angles. Experimental methods are presented which should give improved insight into the mechanism of mechanical erosion by particles harder than the metal surface.

At the institute for Thermal Turbomachinery and Machine Dynamics at the University of Technology in Graz, an *erosion- test rig* was designed for investigating particle impacts for particle sizes of up to 63µm diameter in supersonic velocities up to Mach number 2.2. The Technique of 4- Colour-Schlieren-Visualisation was applied to visualise the flow and the shock pattern. Flow investigation were done using *laser doppler anemometry* (LDA). The measurements were compared to numerical results from an *viscous unsteady flow simulation* performed with the software package FIRE (AVL-Graz, Austria). To examine the impact and restitution angels and particle velocities *laser sheet measurements* as particle image velocimetry (PIV) were used. The *erosion scratches* on the polished specimens were investigated using a scanning electron microscope (SEM). So it was possible to define important parameters of the erosion mechanism and to allow better prediction of erosion rates.

On the bases of theoretical investigations as published before [1] a suggestion of how to correlate impact velocitiy, particle mass and loss of specimen material is presented here. From this more detailed survey (SEM) of specimen volume loss a better correlation of the plowing friction factor with the gas turbine blade metal reality comes into reach. This investigations were done for different particle sizes (1 to 63µm) in the region of small impact angles (around 15°) where severe damage is done to ductile materials.

2. <u>INTRODUCTION</u>

Often in industrial process heat is available in the form of hot gases at **atmospheric pressure level**. A typical example is biomass combustion where the heat is available at ambient pressure level. A novel solution for this case is given in the **inverse gasturbine process [2]** where at first biomass is burned at atmospheric pressure and the hot exhaust gases are conducted to a gas turbine for expansion into

vacuum. At a vacuum pressure of about 0.4bar the gases are cooled in heat exchangers and the moisture content is made to condense. Later on the uncondensable gases are compressed to ambient pressure thus closing the cycle. In those plants we have to handle gases highly loaded with dust particles. The gas turbines which are needed for proper expansion have to be designed as one stage turbines for cost reasons. In that harsh environment of operation with transonic and supersonic flow information about erosion behaviour of blade material is especially important. Erosion can alter blade profiles severely and decrease flow efficiency drastically [3].

Particles elutriated from a fluid bed passing through a gasturbine blading are **continuously reduced in size** due to cracking as consequence of repeated impacts on blade surfaces this has been observed in FCC expanders [4], where the size distribution shows a shift to smaller particle size from inlet towards the exit of the turbine.

It is stated in literature [5] that the value of **material loss** increases with the impact velocity of particles to the power of higher than 2, sometimes even 5 in special cases ($e \sim v^n$ $2 < n < 5$)! Ductile materials like heat- resistant steels show considerable sensibility to **small impact angles** [6] which occur mainly on the blade pressure surfaces.

We hope that the results presented here will form one step closer to the solution of the problem described. The authors will further try to analyse their measurement data in several respects to increase the benefit for the designer.

A further theme of research will be the erosion resistance of **coatings**, as corrosion protecting and also thermal barrier coatings. Coatings of this kind are indispensable for the protection of the high temperature gas turbine blades as described by [7] and [8].

3. GAS FLOW AND SHOCK WAVE PATTERN IN THE EROSION TEST RIG WITHIN A SUPERSONIC CASCADE

3.1. Supersonic Erosion Test Stand

The erosion test stands is designed as a **replaceable cylindrical insert** into the structure of the Transonic- Cascade (**Fig. 3.1-1**). The main parts of the erosion test stand are the wedge-shaped specimen which is attached to an specimen-holder beeing adjustable within the two contour parts. The latter give the channel the needed shape of a naval nozzle. For observing particles in the half depth plane of the 2D-Channel, a **light sheet window** made of glass has to be included in the contour part. This design feature requires a linear part in the continuously curved contour at the position of the leading edge of the specimen. To generate an appropriate mathematically defined contour a B- Spline function was used to guarantee continuity of shape and curvature.
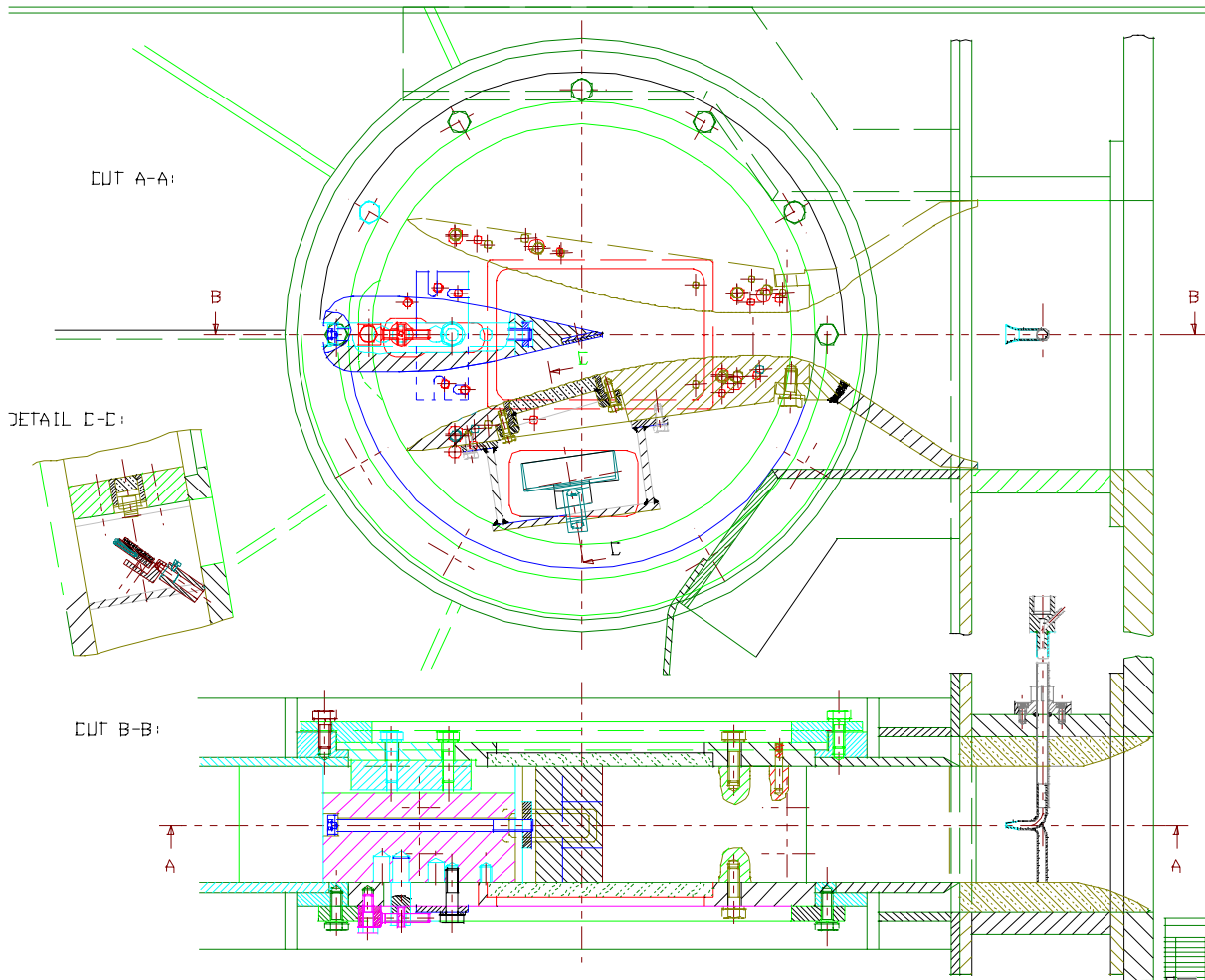
Fig. 3.1-1: **Design Drawing of the Erosion Test Rig**

3.2. 4-Colour- Schlieren- Technique

Parallel light waves passing through a flow field with density gradients are deflected towards the larger value of density. Those **deviated light beams** can be focused afterwards and filtered out at a knife mask, which results in an grey scale image of the gradients in the direction perpendicular to the knife edge. Settles **[9]** improved this technique by colouring the light waves in an diaphragm and used according to the 4 colours 4 knife edges to enable the filtering. With that method **location and gradient orientation** of shock waves could be visualised easily. Unfortunately there is no direct relationship between the brightness and the magnitude of the density gradient.

The **flow pattern around a blunt wedge** (test specimen) in the erosion test stand is characterised by two oblique shock waves which appear nearly parallel on both sides of the specimen (**Fig. 3.2-1**). Using the 4-Colour- Schlieren- Technique both of them can be seen. The detached shock is located a few mm in front of the leading edge and another one starting from the wedge surface. Thus incoming oblique shock wave initiates a local very small separation zone in the boundary layer of the channel contour which causes another oblique shock wave (i.e. reflected one) and an expansion wave to turn the supersonic flow around this tiny obstacle **[10]** or **[11]**. After a short expansion zone another oblique shock wave crosses the channel and raises the pressure level to approximately ambient condition.
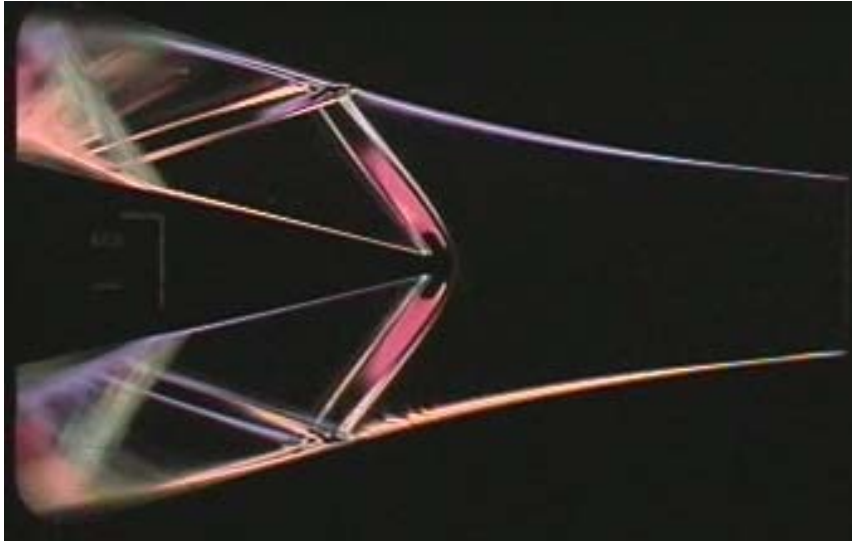
Fig. 3.2-1:   **Shock Wave Distribution At Blunt Wedge**

3.3.   Numerical Simulation With FIRE

The **two dimensional unsteady flow simulation** was done by a finite volume based, pressure correction code for complex flow structures.

The calculated <u>density contours</u> can directly be compared to the Schlieren – pictures, keeping in mind that the latter one visualises gradients. The position of the detached shock wave and the shock reflection on the contour walls are presented.

Downstream to the wedge a considerable unstable <u>recirculation area</u> is present. Its extensions can be appraised on a plot of velocity- vectors. The tiny separation zone and reattachment zone at the position of the reflected shock wave on the lave contour could hardly be seen.
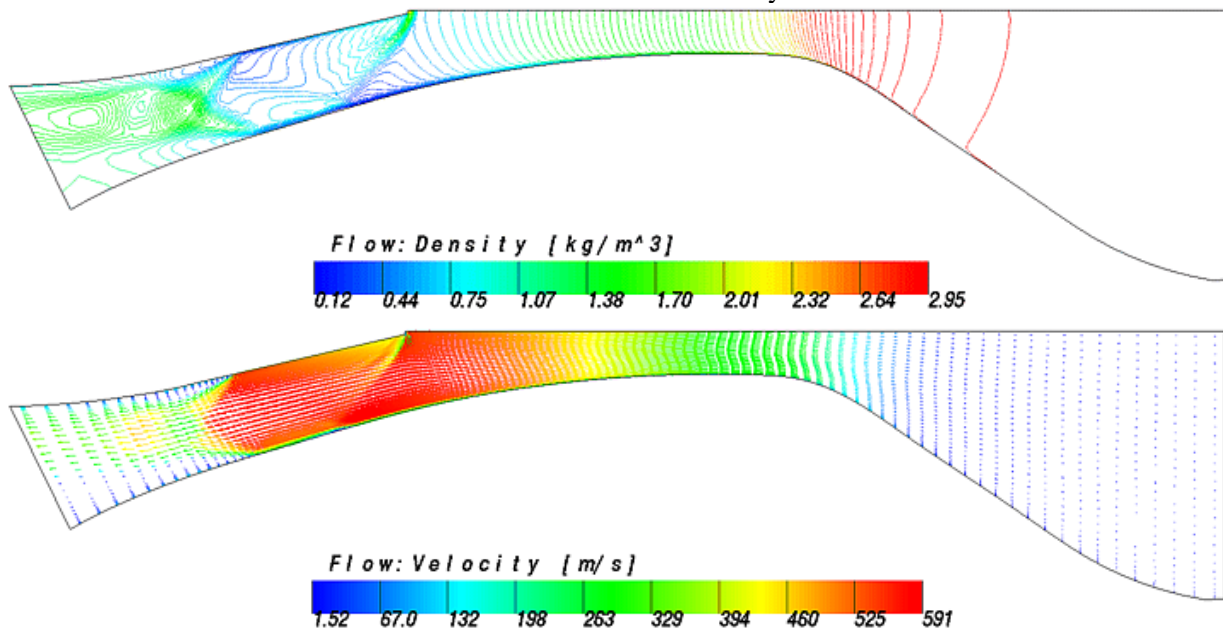
Fig. 3.3-1:   **Flow Calculation Results (FIRE)**

3.4. LDA Measurements

The used DANTEC laser equipment consists of a **twin-ray argon-ion laser** and a Burst Spectrum analyser which examine the signal from the photo-multiplier for evaluating the calculation.

The <u>velocity magnitudes</u> 1.5mm above the surface of the wedge starting at the leading edge as a comparison between LDA and calculation with FIRE show **Fig. 3.4-1.**

For some location along the flow direction two values have been analysed from the LDA- signal according to <u>two distinct peaks</u> which correspond to the fluctuating position of the unsteady second shock wave. The signal upstream to the shock wave position at the leading edge could not be analysed properly. The <u>starting condensation</u> of humidity generates droplets in the range of the applied seeding material of the LDA- system an effect we sought to avoid by raising air inlet temperature.

The extensions of the <u>recirculation zone</u> on the laval cotour pulsates according to the unsteady change of the second shock wave position, which in some extreme situation reaches nearly the location of the first shock wave at the leading edge.
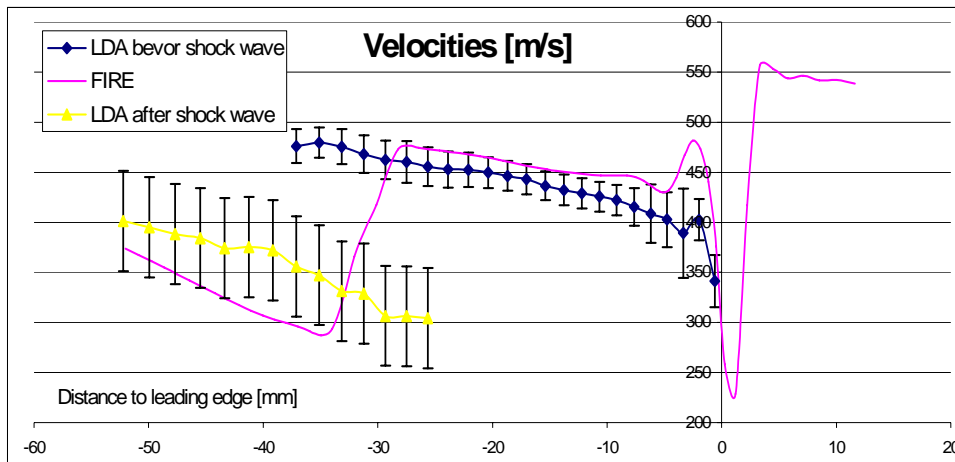
Fig. 3.4-1: Comparison of LDA Measurement and CFD Calculation close to the wedge surface

4. INVESTIGATION OF PARTICLE MOTION AND IMPACT PARAMETERS

4.1. Particle Ingestion

The different experiments conducted required two types of **solid particle injection.** In the case of <u>continuous</u> introduction for the laser measurements a cylindrical tank of approximately 1lit capacity was filled with particles. Compressed air of about 4bar flows through a perforated tube in the centre of this tank and sucks particles into the injection stream. The particles reach the main flow of the test stand through a 90° pipe bent.

To provide an <u>intermitting</u> stream of a distinct amount of particles, the quartz grains are loaded via a funnel directly into the sealed pipe bend, and are afterwards ingested as few by few particles by short duration jet of pressurised air into the main stream.

In both cases the main difficulty is the **agglomeration** effect of particles smaller than 20μm diameter. The particle distribution observed near the leading edge is considerably influenced by the starting conditions of the introduced particles. The **Laval- nozzle focuses** the particles towards its axis, therefore most of them would hit the flat leading edge, and afterwards impact several times on the specimen surface. To force the particles to hit the surface **directly on the specimen** in its inclined position behind the leading edge the ingesting pipe bend was inclined -15° to the axial direction. Another severe effect for the radial deviation of the particles in the main stream is the different inertia force due to the **acceleration within the ingesting pipe** bend which tended to deviate the particle sidewise.

Nevertheless, the direction of the first impact on the surface <u>do not differ very much</u> from the axial direction.

4.2. <u>PIV Measurements</u>

For evaluating the erosion phenomena the **impact velocities** and **angles** are of special interest. Therefore, the very advanced PIV-method has be applied using a <u>double pulse ruby laser.</u> The laser is optically widened to a horizontal <u>light sheet</u> which is deflected via a mirror and a window in the lower LAVAL- contour part in the mid plane of the 2D channel. Particles moving along the light sheet deflect light in perpendicular direction where a camera is located to expose a photographic film. They are displayed twice, according to the pulse delay (2 to 5µs). The photo- camera was equipped with an exchangeable CCD-chip to enable optimal adjustment very close to the surface.

The PIV-images are enlarged 5 times during the photographic developing procedure and digitised afterwards for being used in an **automatic analysis** (**Fig. 4.2-1**). An <u>auto-correlation procedure</u> computes the correlation values for every interrogation area subsequently for the whole PIV image. The program select the three most probable correlation direction out of the correlation field. Finally, an validation procedure figure out the most realistic velocity vector by comparing adjacent vectors and applying other selecting criteria.

interrogation area

correlation field

0.8 mm

300 m/s

original PIV image

final field of velocity vectors
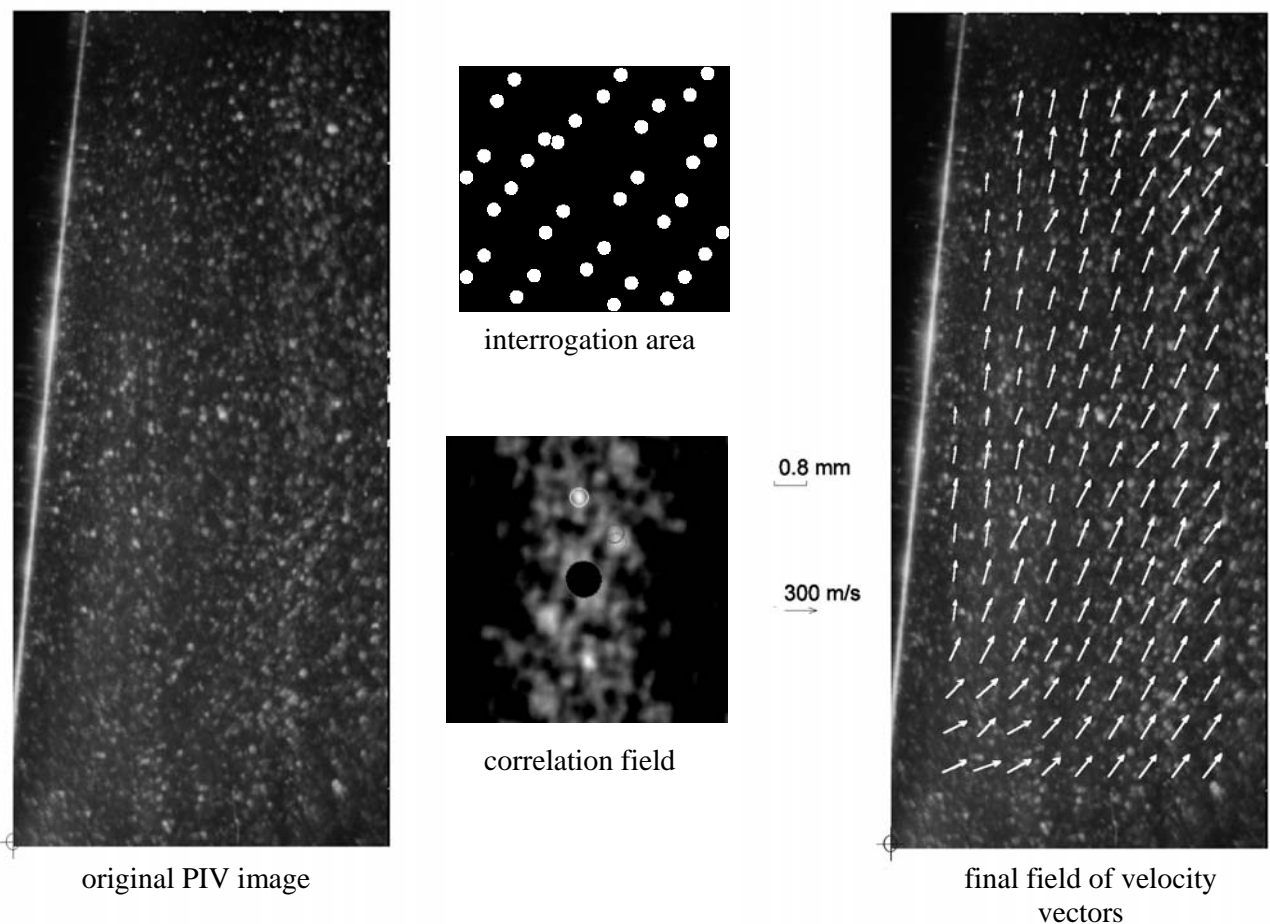
Fig. 4.2-1:   Steps in PIV Analysis Procedure

After a statistical analysis of all different calculations and averaging the significant values of all CFD calculations they could be compared to the PIV measurements as shown on **Table 1.**

particle size	PIV measurement					
	v_min	v_average	v_max	α_min	α_average	α_max
μm	m/s	m/s	m/s	°	°	°
10-25	352	**388.7**	430	8	**10.0**	12
25-40	267	**292.8**	321	8	**11.0**	13
40-63	182	**222.5**	265	6	**9.0**	12
	Calculated Results (FIRE)					
5.0	441	**448.5**	454	6	**7.7**	9
10.0	415	**418.1**	421	11	**11.3**	12
17.5	368	**369.2**	371	12	**12.7**	13
25.0	333	**335.3**	338	12	**13.2**	14
32.5	306	**307.0**	309	12	**12.9**	14
40.0	284	**285.4**	287	11	**12.4**	14
51.5	264	**267.2**	270	10	**10.5**	12
63.0	240	**240.2**	240	11	**11.7**	12

Table 1: Comparison Of Calculated And Measured Impact Parameters

From the results of the PIV measurements *rebound coefficients* for different particle sizes as shown in **Table 2** could be derived easily as ratio of according rebound to impact value.

particle size	v_min	v_average	v_max	α_min	α_average	α_max
	m/s	m/s	m/s	°	°	°
10-25	0.71	**0.76**	0.79	0.73	**0.81**	0.85
25-40	0.79	**0.88**	0.90	0.63	**0.79**	0.92
40-63	0.91	**0.98**	1.01	0.71	**0.97**	1.09

Table 2: Rebound Coefficients for different particle size

4.3. Calculated Particle Trajectories

The influence of the **introduction parameters** on the impact position at the specimen has been investigated on trajectories for 5 different *starting locations* and 5 different *starting angles*. (As a means to simulate the variation in particle starting conditions in reality.) There are different starting velocities for every particle size, considering the distinct particle acceleration in the ingestion duct itself.

The *deviation* in the particle trajectories due to different starting location are shown on **Fig. 4.3-1** for particles with diameters of 5µm. Larger particles show smaller differences between trajectories from different starting position.

The influence of starting angles (+/- 10°) on impact position on the specimen is very small. The trajectories form smaller particles could not be separated. The **focusing effect** of the Laval nozzle is obviously strong due to low starting velocities especially for bigger particles.

9 particle sizes (1,5,10,17.5,25,32.5,40,51.5,63µm) have been selected to compare the **inertia effects** on the different particle trajectories. On the according particle velocities more details about the differences in acceleration after ingestion and at impact position on the wedge are presented. Negative Velocities indicate the flow from right to left.
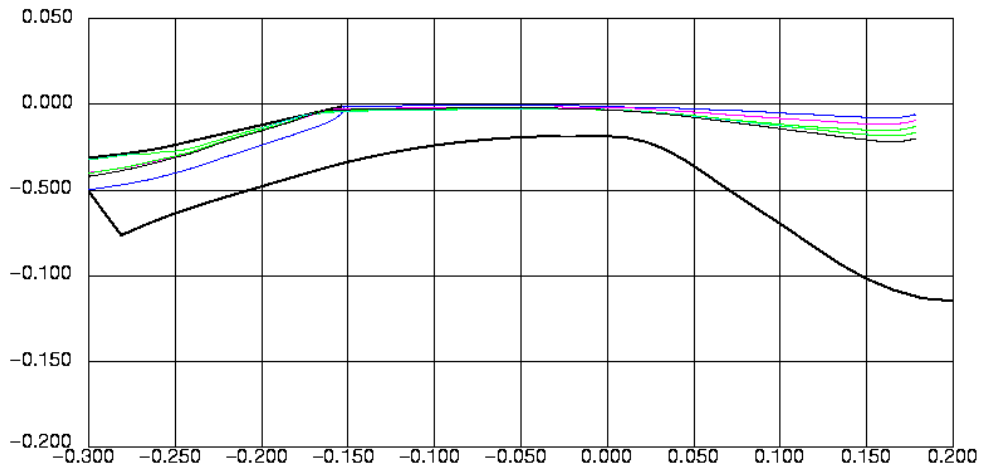
Trajectories for particles of 5µm diameter started from 5 different positions
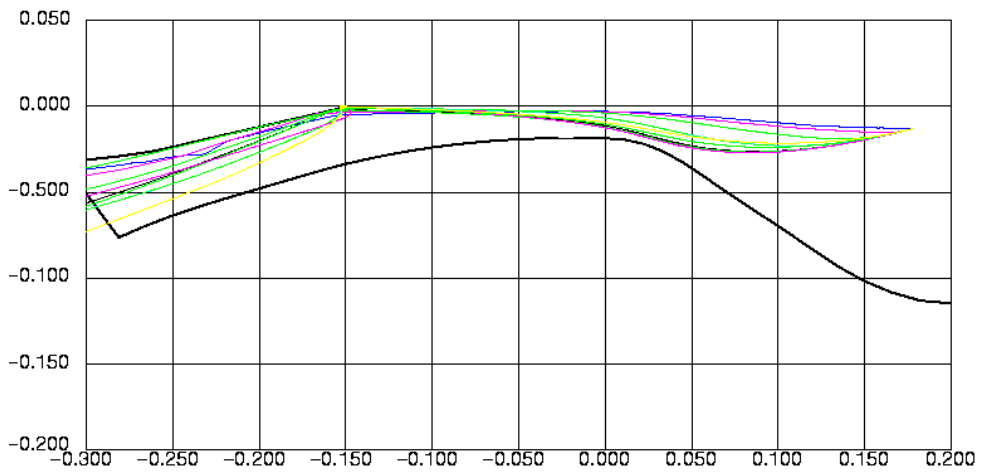
Trajectories for 9 particles with different size started from the identical position
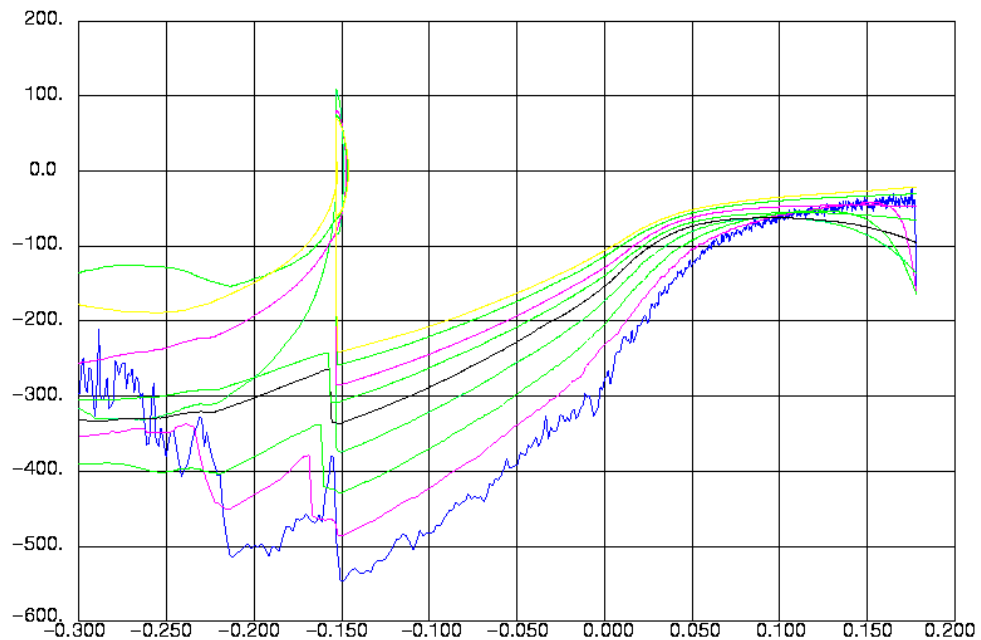
Particle velocities for 9 particles with different size started from the identical position

Fig. 4.3-1:   Calculated Particle Trajectories and Particle Velocities

5. ELECTRON-MICROSCOPICAL ANALYSIS OF EROSION PATTERNS ON THE SURFACES OF THE SPECIMEN

5.1. Scanning Electron Microscope

A beam of electrons is shot on a distinct point on the specimen and set electrons free from the metal surface. The number of the detected secondary electrons define the brightness of that particular point on the image. As more electrons are released from edges and corners than from a plain or an concave region a perfect criteria for generating best spatial pictures with optimum depth of focus is given.

Thus, the SEM images provide us the possibility to understand the microscopic erosion mechanism of particles with supersonic speed.

5.2. Theory Of Abrasive Material Loss Due To Single Particle Impact

Due to differences in hardness of the erodent and the **ductile** target material the particle edges usually penetrate the metal surface. Severe erosion could be observed at angles around 15 to 30 degrees by scratching and cutting mechanisms. Plowing of particle edges is often observed together with breaking of edges. It is stated in literature **[12]** that the criteria for big material loss from smallest particles is stress fatigue by repeated particle impacts. Due to elastic properties they are very resistant against perpendicular impacts.

Whereas **Brittle** materials suffer most from that perpendicular impacts. These generating cracks below the metal surface which leads to material loss in form of flat plates. The dimension of those flat plates could exceed the diameter of the impacting particles **[13]**.

5.3. Erodent Material

Dried **Quartz-powder** ZE 36 1600 from *Quarzwerke Zelking* (density 2650kg/m^3) was used as eroding material. A tendency to **agglomeration** due to intermolecular forces are readily apparent at particle diameters lower than 20μm.

On each specimen **1g of quartz sand** with defined range of size has been shot.

For the majority of the particles the break-up criteria (tensile strength due to bending moment at impact) has been reached.

5.4. Erosion Specimen

The specimens used for analysing the scratches after being exposed to the supersonic particle impacts, are flat plates in dimensions of 35x40x2mm of blade material (X20CrMoV12-1 [DIN 17175; 1.4922]). They were fixed on the lower leg of the Erosion wedge in the middle axis of the nozzle.

On every specimen **4 impact regions** have been investigated with different densities of particle impacts. The closer the region to the leading edge and the closer to the middle axis, the more particle impacts per mm^2 could be observed. Therefore two positions close to the leading edge of the wedge have been chosen with different distances to the middle axis (2mm and 18mm). Two according locations at a distance of about 25mm to the leading edge have been added.

To figure out the influence of the particle size **3 different sizes of particles** have been introduced.

5.5. Erosion Pattern

Differences in the **location** of scratches on the probe surface is mainly due to the number of impacts which is of course variable in the length and width of the specimen. The scratches seem to indicate that impact velocities and angles do not differ significantly, although towards the leading edge the *density of impacts* increases. Since the particles are ingested into the symmetry plane of the channel particle impacts probability towards the side walls decrease (Gaussian distribution).

Some **typical shape** of erosion scratches could be divided. *Long scratches* (above one diameter in length) indicate direct material loss by cutting metal chips (estimated as one tenth of an particle diameter in height). In some impact conditions the particles could not directly remove material but *plough* through the metal surface. Repeated impacts of this kind cause stress fatigue and therefore material loss on long-term.

Circular small dots with small penetration depths indicate the contact of single particle edges and lead not directly to erosion but deform the metal surface. In most cases there remain a part of the attacking particle sticking in the surface.

Curved scratches may arise due to single sharp edges penetrating the metal surface being in eccentric location at particle outer surface, thus turning the particles sidewise as well as rolling it in the direction of impact.

According to the **size of the particles** different dimensions and a slightly change in the shape of the erosion pattern could be observed. **Fig. 5.5-1** present a comparison of SEM pictures of specimen suffer on different particle size impacts (10-25μm respectively 40-63μm). The different magnification is listed in the bottom left corner of the pictures. To illustrate the dimensions a size bar is added. The main flow direction is from bottom to the top of the image.

For larger particles the penetration depth and width of the scratches seems to be relatively larger than those of smaller particles. More broken edges of particles remain in the specimen shot with bigger particles. The number of small particle impacts decrease with particle size.

| 10-25μm | 40-63μm |
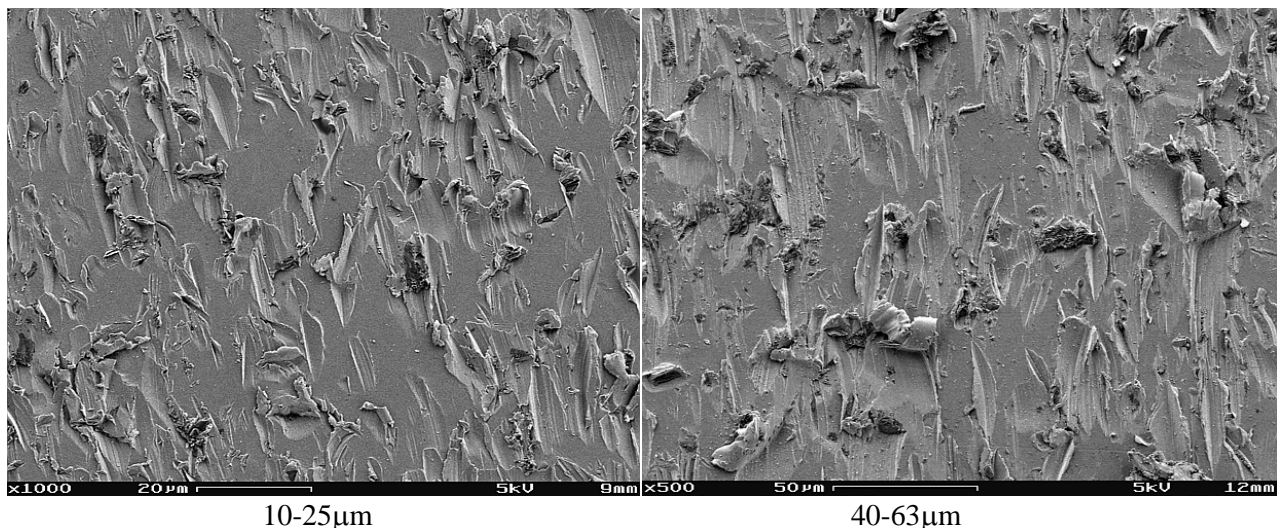
Fig. 5.5-1: SEM Picture Of Different Erosion Scratches

5.6. Material Loss

The electron-microscopic analysis of erosion patterns enabled the authors to roughly estimate a average volume loss at single impact. This was done baring in mind the measured impact velocities and impact angles of the particles and providing thus the necessary correlation for the theory already put forward. As a first result the **mean values** are shown in the following **Table 3**. The correlation of average values of impact velocity to average value of metal loss at single impact has thus be established.

particle size μm	v_average m/s	α_average °	kin Energy 1E6kgm^2/s^2	scraped Volume 1E-18 m^3
10-25	388.7	10.0	0.35	16.1
25-40	292.8	11.0	3.90	39.8
40-63	222.5	9.0	8.96	96.4

Table 3: Average Material Loss Due to Single Particle Impacts

6. CONCLUSIONS

- A quite good agreement between measurements and CFD calculation could be achieved for the case of flat angle impact on ductile metal specimens.
- Single impact of particles leads to scratches which make the impression of ploughing the hard particle edges through the more soft metal surface. Thus tilted up side walls of ductile materials are generated which have to be counted as erosion loss since impacting smaller particles will remove them easily by fatigue bending.
- It can be sated that at these high velocities particles are prone to cause extreme damage.
- Severe erosion damage occurs due to stress fatigue on repeated impacts of the higher number of small particles.
- Most of the particles break apart at impact or lose broken edges which remain stuck in the metal even at small impact angles.

7. ACKNOWLEDGEMENT

8. REFERENCES

[1] Jericha, H., Göttfried, T., Sanz, W., 1989, "Industrial gas turbine blade erosion", ASME Cogen Turbo, IGTI 4, 193-200

[2] Fesharaki, M, Halozan, H., Jericha, H., Kulhanek, G., 1997, "Biomass-Fired Atmospheric Gas Turbine Plant-I", ASME Turbo Expo 97, Orlando, Florida, ASME paper 97-GT-290

[3] El-Sayed, A. F. A. A., Brown, A. 1987, "Computer Predictions of Erosion Damage in Gas Turbines", ASME 87 GT 127

[4] Bauer, E., and Jericha, H., 1987, "Refinery FCC Plant Energy Recovery 75000h of cyclone and expanding gas turbine", CIMAC Warsaw, T-1

[5] El-Sayed, A. F. A. A., 1995, "Prediction of Erosion in Pipe Bends Due to Particulate Flow", Engineering Research Journal Vol. 4 of University of Helwan, ISSN 1110-2330

[6] Kotwal, R., Tabakoff, W., 1981, "A New Approach for Erosion Prediction Due to Fly Ash", Journal of Engineering for Power Vol. 103

[7] Elsner, W., 1998, " Schäden im Heißgaspfad von Gasturbinen und ihre Ursachen", Allianz Report 2/1998

[8] Tabakoff, W, Metawally, M., Hamed, A., 1993, "High Temperature Coatings For Protection Against Turbine Deterioration", ASME Cogen-Turbo, IGTI-Vol.6

[9] Settles, G., 1970, "A Four-Colour Schlieren Technique With Sensitivity In All Directions", Tennessee Engineer, pp. 4.5. 7-9

[10]   Shapiro, A., " The Dynamics and Thermodynamics of COMPRESSIBLE FLUID FLOW", The Ronald Press Company , New York

[11]   Sieverding, C. H., 1976, "Transsonic Flows in Axial Turbomachinery", Von Karman Institute for Fluid Dynamics

[12]   Zum Gahr, K.H., et. al., 1983, "Reibung und Verschleiß", Deutsche Ges. für Metallkunde

[13]   Watanabe, S., 1985, "Erosion Studies With Fluid Catalytic Cracking Catalysts" ASME

WORK TO BE DONE

- **Tables**

- **Diagrams**

- subsonic – supersonic differences (zum Gahr, **Ghanimi**, El-Sayed, Tabakoff)
- **Others**
  - actualise References
  - break-up kriteria []
  - e-mail concerning number of illustrations, format restrictions for review process, how to supply pictures for final version to be printed (inserted in the text, single files, hardcopies, photos)

PIV, bzw. TRACING Polarisationsfilter vor FOTO-Kamera➔ zur Ausfilterung von schrägem Streulicht bewirkt nur geringe Verbesserungseffekte

Prof. Staudinger: according to the change of form of sand grains, he mentioned that the reduction of sizes happens according to faults in the crystalline structure, and therefore the break up energy will increase with smaller diameter, and the edges should therefore be **sharper with smaller diameter** (Pö replied: my contrary statement given before was found during observation the particle distribution and are not verified with measurements. Jericha: insisted to remember this shapes from former investigations of the catalysts of an FCC plant with mainly SiO_2 particles)

8.1.   Abrasive Material

The images of single **Quartz**-grains (Quartz-powder ZE 36 1600 of *Quarzwerke Zelking* (density 2650kg/m^3) as eroding material give an idea of the irregular shape of the particles and show the tendency of bigger and sharper edges with increasing diameter Fehler! Verweisquelle konnte nicht gefunden werden.**.** A tendency to **agglomeration** due to intermolecular forces are readily apparent at particle diameters lower than 20µm! On each specimen **1g** of quartz sand with defined size has been shot.

For the majority of the particles the break-up criteria (tensile strength due to bending moment at impact) has been reached.

Fig. 8.1-1: **Shape Of Quartz Grains Of Different Sizes**

8.2. Particle Path

To detect particle path and impact and rebound angles a **particle tracing method** was used. To achieve this, a horizontal light sheet is deflected via a mirror and a window in the lower LAVAL-contour part in the mid plane of the 2D channel. Particles moving along the light sheet deflect light in perpendicular direction where a camera is located to expose (2 to 5µs) an photographic film. This method visualises the path of single particles as long as they remain in the light sheet.

Incidence and rebound angles have been deduced at several distances from the leading edge of the specimen, but do not vary much with the location. The trend of the influence of the particle size, could be estimated. (The bigger a particle, the smaller is the difference in the rebounding angles). A Gaussian distribution curve could be superimposed to analyse the average angle.

[5]   Tabakoff, W., und Hamed, A., 1987, "Temperature Effect on Particle Dynamics and Erosion in Radial Inflow Turbine", ASME Paper 87-GT-123

[9]   Jericha, H., Sanz, W., und Pöschl, R., 1995, "Industrial Gas Turbine with High Rate Particle Flow", ASME Cogen Turbo,Wien

[10]   Zettl, E., Jericha, H., 1995, "Staubströmung in thermischen Turbomaschinen (Teil 2: Partikelbewegung in Grenzschichten)", ÖIAZ Sonderband 10-11/95 O/170

 Bölcs, A., and Sari, O., 1988, "Influence, of Deposit on the Flow in a Turbine Cascade", ASME Paper 88-GT-207

 Elfeki, S., and Tabakoff, W., 1986, "Erosion Study of Radial Flow Compressors with Splitters", ASME Paper 86-GT-240

Tabakoff, W., 1980, "Study of metals erosion in high temperature coal gas stream", Transaction of the ASME

Tabakoff, W., Hamed, A., and Metwally, M., 1991, "Effect of Particle Size Distribution on Particle Dynamics and Blade Erosion in Axial Flow Turbines", ASME Paper 90-GT-114